

**Control chart pattern recognition under small shifts based on multi-scale weighted  
ordinal pattern and ensemble classifier**

Yazhou Li<sup>a</sup>, Wei Dai<sup>a,1</sup>, Yihai He<sup>a</sup>

<sup>a</sup> School of Reliability and Systems Engineering, Beihang University, Beijing 100191,  
China

**\*Corresponding authors at:**

School of Reliability and Systems Engineering,

Beihang University

No. 37 Xueyuan Road,

Haidian District, Beijing, 100191, P.R. China,

Wei Dai, E-mail address: dw@buaa.edu.cn

Tel.: +86-13810584286

---

<sup>1</sup> Corresponding author. Tel.: +86-13810584286. E-mail address: dw@buaa.edu.cn (Wei Dai).

## **Acknowledgements**

This work is supported by the National Defense Basic Scientific Research program of China (JSZL2022213B001).

## **Declaration of Competing Interest**

The authors declare that they have no known competing financial interests or personal relationships that could have appeared to influence the work reported in this paper.

# **Control chart pattern recognition under small shifts based on multi-scale weighted ordinal pattern and ensemble classifier**

## **Abstract**

Production orientated toward high-quality products makes the manufacturing process highly accurate and precise with minimal variations in its parameters. Accurately identifying small variations in critical control points is extremely important in quality control. The existing control chart pattern recognition (CCPR) methods usually focus on the moderate and large shifts to detect anomalies of pattern parameters, yet ignore the effects of small shifts. Moreover, traditional features only consider the magnitude characteristics of the control chart pattern (CCP) data, and ignore all other characteristics. To solve these problems, a new feature and multi-scale ensemble classification model is proposed in this paper. First, the ordinal pattern (OP) features based on the sequential characteristics of CCP data and the weighted OP (WOP) features combining sequential and magnitude characteristics are proposed. Second, an ensemble classification model (WOP-EC) based on multi-scale WOP features is constructed. Simulation results show that the correct recognition rates of WOP-EC are 94.31% and 99.88% under small and large shifts, respectively. Compared with other traditional features, WOP-EC has better recognition performance under different window sizes and separability levels and can greatly reduce the two types of error.

## **Keywords:**

Control chart pattern recognition; Ordinal patterns; Multi-scale WOP feature; Ensemble Classifier; Small Shifts

## **1. Introduction**

Statistical process control (SPC) methods are used to monitor manufacturing processes in industrial settings to ensure process stability and improve product quality. The control chart is an important tool in SPC for quickly detecting process variations and the occurrence of assignable causes (Cuentas et al., 2022). A timely detection of these causes is necessary to apply the corrective actions and reduce the number of defective products (Lee et al., 2022)).

Manufacturers must continuously improve their processes and product quality to maintain their competitive edge (Chen et al., 2020). When the process is improved to a certain level, fluctuations in the quality of a product will be further reduced (Baik et al., 2011). This process is known as high-quality process (HQP), which requires a high degree of accuracy and precision in the manufacturing process, especially in the aerospace and electronics industries (Alwan et al., 2023). HQP monitoring data show small variations as evidenced by the small mean shifts in these data and the small shifts in the pattern parameters generated by anomalies. Therefore, HQP requires highly sensitive monitoring methods to capture small changes in critical control quantities during the manufacturing process.

Traditional control charts with control limit monitoring methods cannot easily achieve accurate process monitoring and assignable cause identification of small shifts and have high false alarm rates (Ali et al., 2016). Shewhart control charts are mainly used to monitor large shifts in the process and are less sensitive to small and moderate shifts (Mughal et al., 2018). Cumulative Sum (CUSUM), Exponentially Weighted Moving

Average (EWMA) control charts, and improved control charts based on CUSUM and EWMA are widely used to capture small shifts in HQP (Yeong et al., 2021). However, these control-chart-based monitoring methods rely on control limit accuracy, their results only determine whether the process is in control or not, and they do not allow a timely identification of assignable causes. In addition, CUSUM and EWMA control charts are influenced by historical data, and the monitoring results are dependent on the parameter settings.

With the development of artificial intelligence (AI) and computer technology, intelligent manufacturing has become the future trend of manufacturing. Control chart pattern recognition (CCPR) is a quality control method that combines AI with control charts (Yeong et al., 2021).

The control chart pattern (CCP) is a set of time series. The Western Electric Company (Company, 1958) lists 15 common CCPs, of which normal pattern (NOR) indicates a controlled pattern. Among these patterns, cyclic (CYC), upward trend (UT), downward trend (DT), upward shift (US), downward shift (DS), systematic (SYS), and stratification (STR) are the most common abnormal patterns, as shown in Fig. 1. These abnormal CCPs are usually associated with a set of potentially assignable causes that affect product quality and cause specific manufacturing defects (Li et al., 2023). For instance, tool wear and equipment degradation can cause trend patterns, while CYC is often associated with cyclic changes in temperature and power supply (Addeh et al., 2018).

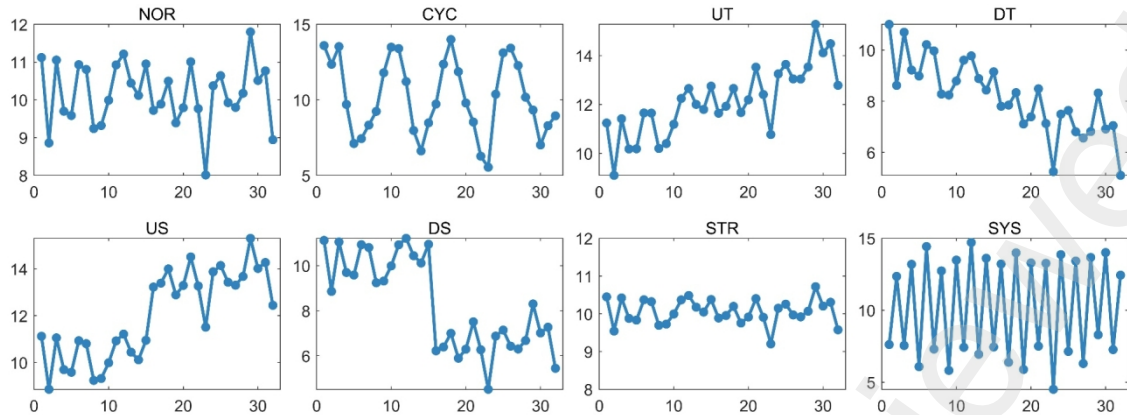


**Fig. 1.** Eight different CCPs.

The input is a key area in CCPR research and many studies have taken unprocessed raw data as their input (Al-Ghanim and Ludeman, 1997; Zan et al., 2020). While this method eliminates the need for data preprocessing, having a very large input will increase the complexity of the classifier structure, reduce the speed of operation, and is not conducive to the real-time processing of massive data (Aziz Kalteh and Babouei, 2020; Ranaee et al., 2010). Features extracted from raw data can characterize the different attributes of CCPs, reduce model size and improve recognition performance (Xue et al., 2023). Common features include shape features (Ebrahimzadeh et al., 2013; Gauri and Chakraborty, 2006, 2009; Pham and Wani, 1997), statistical features (Hassan et al., 2003), and wavelet features (Al-Assaf, 2004). Chiu et al. (2021) studied a mix of statistical and shape features and successfully identified most concurrent CCPs with an accuracy of 91.8%. With the development of machine learning (ML), many new CCPR classifiers have been proposed, but feature improvements for CCPs are relatively few.

The abovementioned traditional features focus only on the magnitude characteristics of CCP data and ignore the order relationship of the sampling points. In practical industrial applications, magnitude-based features are easily affected by outliers (Li et al.,

2023). In addition, traditional features mostly represent the global information of the time series and ignore the detailed fluctuations and local variations in the data (Bandt, 2019). For these reasons, the values of magnitude-based features may be similar for different types of CCPs, and the detail fluctuations play key roles in distinguishing these CCPs. Therefore, the accuracy of CCPR should be improved by identifying the detail fluctuations of the sampling points within a specific window.

Ordinal pattern (OP), as a symbolic time series analysis method, has been widely used in the meteorological, medical and mechanical fields in recent years (Kulp and Zunino, 2014; Landauskas et al., 2020; Wang et al., 2016). Introduced by Bandt and Pompe (Bandt and Pompe, 2002), OP analysis describes the sequential relationship between a limited number of points in a time series without considering the numerical value itself, and is less infected by noise or outliers. The basic assumptions of OP are that the underlying structure and information of a time series are composed of repeating basic fluctuation units (i.e., OPs) and that the OPs of different state time series show some variability (Li et al., 2023). Following these assumptions, CCP samples can be converted into a finite number of OP features. CCP follows a particular OP distribution under specific scale parameters, and the OP distribution shows large differences under different observation scales. Weiß et al. (2023) proposed a nonparametric control chart based on ordinal patterns that does not rely on distributional assumptions and observes a sequential dependence in the data. However, OP features only consider the order relationship between the data and ignore the data magnitude. In this paper, a weighted ordinal pattern (WOP) feature based on data magnitude is proposed by combining these two

characteristics. Given that the WOP features obtained at a single observation scale do not contain comprehensive information, multi-scale WOP features are further constructed.

In addition to model inputs, ML-based classifiers are also key to improving the performance of the CCPR model. Artificial neural networks (ANN) were first used in CCPR(Al-Ghanim and Ludeman, 1997;Pham and Wani, 1997). Subsequently, support vector machines (SVM) (Ranaee et al., 2010), random forests (RF) (Chiu and Tsai, 2021) and other methods have also demonstrated a strong CCP classification performance. Lee et al. (2022) proposed a model based on the spectral clustering technique with SVM to achieve CCP classification under gamma distribution. Deep learning models have also been used for CCPR and have demonstrated a better performance than traditional neural networks. Maged et al. (2023) proposed a variable window size convolutional neural network (CNN) model for CCPR that achieved 99.78% correct recognition rate. Ünlü (2021) constructed a cost-oriented long and short-term memory networks (LSTM) model that outperforms SVM in terms of classification and early detection. Despite achieving excellent results, deep learning requires much time to adjust the parameters and train the model (Kanjilal and Uysal, 2021). In addition, individual classifiers (IC) may have certain attribute bias in recognition, thus leading to classification errors. Ensemble classifier (EC) combines the recognition performance of multiple ICs, to significantly improve their scheme recognition ability and compensate for the limitations of ICs (Alwan et al., 2023; Hassan, 2008). Ensemble classification can also combine the multi-scale characteristics of WOP features to construct a multi-scale EC model, which is conducive to improving the CCP recognition performance.

Most of the current CCPR methods only classify CCPs at moderate and large shifts yet ignore the small shifts in the HQP. This paper aims to address the abovementioned challenges and the limitations of traditional features that only consider magnitude properties. To this end, a new multi-scale WOP feature is proposed and combined with ensemble classification to construct a WOP-EC model. The contributions of this work are summarized as follows:

- (1) In response to the problem where traditional features contain only magnitude characteristics, OP features based on the sequential characteristics of CCP data are constructed. To the best of the authors' knowledge, this study is the first time to construct features from the perspective of the order relationship of sampling points in CCP.
- (2) A WOP feature that fuses two characteristics, namely, magnitude and sequential, is proposed. Experiments show that the WOP feature can accurately identify eight types of CCPs and effectively reduce Type I error and Type II error. The recognition performance of the WOP feature is significantly higher than that of other traditional features under small shifts in the HQP.
- (3) The proposed WOP-EC ensemble classification model integrates the CCP information under different observation scales, thus proving its strong adaptability and robustness across different application scenarios. The WOP-EC model achieves a 99.88% correct recognition rate when the CCP window length is 32.

The rest of this paper is structured as follows. Section 2 describes the proposed method in this paper, including the CCP simulation method for small shifts, the WOP features, and the multi-scale ensemble classification method. Section 3 verifies the performance of

the proposed method through simulation experiments. Section 4 analyzes and discusses the experimental results. Section 5 concludes the paper and proposes future research directions.

## 2. Methodology

### 2.1 Simulation method of CCPs for small shifts

The advancements in automation and sensing technologies have effectively facilitated the collection of process data. However, classifying and labelling large amounts of process data is time consuming, and collecting anomaly data in the field is difficult and costly (Xue et al., 2023). Therefore, various CCP data are usually obtained by Monte Carlo simulation based on the distribution of sufficiently controlled process data. Each CCP has three main components, namely, controlled process mean, random noise, and specific pattern interference, which are expressed as follows (Li et al., 2023):

$$y_t = \mu + x_t + d_t \quad (1)$$

where  $y_t$  is the  $t$ -th process observation, the constant term  $\mu$  is the controlled process mean.  $x_t = r_t \times \sigma$  is the random disturbance of the process following the normal distribution  $x_t \sim N(0, \sigma)$ ,  $\sigma$  denotes the standard deviation of the controlled process, and  $r_t$  is a random quantity following the standard normal distribution at time  $t$  that denotes the chance fluctuation.  $d_t$  is used to simulate specific abnormal patterns and  $d_t = 0$  represents the NOR that is only subject to random disturbances. Table 1 summarizes the formulations and common parameter ranges of the eight CCPs.

**Table 1.**

The formulation and common parameter ranges for generating the eight CCPs.

| <b>Pattern</b> | <b>Standard equations</b>                   | <b>Parameters</b>           | <b>Parameter range</b>               |
|----------------|---|-----------------------------|--------------------------------------|
| NOR            | $y_t = \mu + x_t$                           | Mean value $\mu$            | /                                    |
|                |   | Standard deviation $\sigma$ | /                                    |
| CYC            | $y_t = \mu + x_t + a \times \sin(2\pi t/T)$ | Amplitude $a$               | $a \in [1.5\sigma, 2.5\sigma]$       |
| UT             | $y_t = \mu + x_t + g \times t$              | Period $T$                  | $T \in [4, 6, 8, 10, 12]$            |
| DT             | $y_t = \mu + x_t - g \times t$              | Slope $g$                   | $g \in [0.05\sigma, 0.10\sigma]$     |
| US             | $y_t = \mu + x_t + v \times s$              | Shift position $v$          | $v \in [N/2-4, N/2-4]$               |
| DS             | $y_t = \mu + x_t - v \times s$              | Shift magnitude $s$         | $s \in [0.1\sigma, 0.3\sigma]$       |
| STA            | $y_t = \mu + r_t \times \sigma'$            | Random noise $\sigma'$      | $\sigma' \in [0.2\sigma, 0.4\sigma]$ |
| SYS            | $y_t = \mu + x_t + h \times (-1)^t$         | Systematic departure $h$    | $h \in [1.0\sigma, 3.0\sigma]$       |

where  $N$  is the window length of CCPs that usually contains 16 to 64 observations. In this paper, the window length is set to  $N = 32$ , and the effects of different window lengths  $N$  on model recognition performance are compared.  $T$  is the period parameter of the CYC,  $v$  is the shift position parameter of shift patterns (equals 0 and 1 before and after the shift, respectively). The mean  $\mu$  and standard deviation  $\sigma$  are determined by the actual controlled process. To make the simulated data close to the real situation, the rest of the CCP parameters are randomized within the given range.

Only a few CCPR studies have explored pattern parameter identification under small shifts in the HQP. Their findings show that the values of abnormal pattern parameters are highly variable and greatly affect the recognition results of the CCPR model (Barghash and Santarisi, 2004). Maged et al. (2023) found that smaller pattern parameters result in severe Type I error and Type II error, leading to lower correct recognition rates. Ünlü (2021) demonstrated that the recognition performance of the CCPR model significantly decreases along with decreasing pattern parameter values. Yu et al. (2009) investigated the recognition results for CCPs with different parameter ranges and obtained poor results

when dealing with small shifts. The pattern parameter ranges for generating CCPs in recent works are summarized in Table 2.

**Table 2**

The pattern parameter ranges for generating CCPs in recent works.

| Study                           | CCP parameters (Pattern type) |              |              |                 |            |
|---------------------------------|-------------------------------|--------------|--------------|-----------------|------------|
|                                 | $a$ (CYC)                     | $g$ (UT/DT)  | $s$ (US/DS)  | $\sigma'$ (STA) | $h$ (SYS)  |
| (Xue et al., 2023)              | [1.5, 2.5]                    | [0.05, 0,10] | [1.5, 2.5]   | /               | /          |
| (Maged and Xie, 2023)           | [1.5, 4.0]                    | [0.10, 0,30] | [1.5, 3.0]   | /               | /          |
| (Lee et al., 2022)              | [1.5, 3.0]                    | [0.05, 0,10] | [1.5, 3.0]   | /               | [1.0, 3.0] |
| (Aziz Kalteh and Babouei, 2020) | [1.5, 2.5]                    | [0.05, 0,10] | [1.5, 2.5]   | [0.2, 0.4]      | [1.0 ,3.0] |
| This study                      | Small shifts                  | [0.5, 1.5)   | [0.02, 0,04) | [0.5, 1.5)      | [0.5, 1.5) |
|                                 | Moderate shifts               | [1.5, 2.5)   | [0.04, 0,08) | [1.5, 2.5)      | [1.5, 2.5) |
|                                 | Large shifts                  | [2.5, 3.5]   | [0.08, 0,12] | [2.5, 3.5)      | [2.5, 3.5] |

Most of the methods adopted in the literature only focus on the CCP pattern parameters for moderate and large shifts, and ignore the effect of small shifts on the CCPR model. To address this gap, the pattern parameter ranges of different CCPs are classified into three intervals, namely, small, moderate and large shifts, according to their separability level. The recognition performance of the proposed method is then evaluated across different intervals, especially in small shifts.

## 2.2 Basic principle of OP analysis

### 2.2.1 OP features

OP reflects the scale information of CCPs under specific parameters by describing the inherent order fluctuations of the data within a given length. In this study, OP probability distributions are used as features that represent the attributes of different CCPs. The OP features characterize the original CCP data from the perspective of sequential relationship

and have a small information subspace, which helps to improve the CCPR recognition rate.

The OP analysis divides the sequence  $Y$  into multiple subsequences of length  $m$  and sampling interval  $\tau$  by parameters  $m$  and  $\tau$  and then maps these subsequences to the corresponding  $m$ -order OPs.  $\tau$  is the time delay parameter that indicates the observation scale of the OP features, and  $m$  is the embedding dimension parameter that determines the type and length of OP features. The parameter  $m$  ( $m \geq 2$ ) corresponds to  $m!$  kinds of OPs, denoted by  $\Pi^m$ . Each OP represents a permutation of the positive integers 1 to  $m$  (Berger et al., 2019), denoted by  $\Pi^m(k)$ ,  $k = 1, 2, \dots, m!$ .  $m$  is usually discussed in the range [2,6]. When  $m = 2$ , there exist only two OPs, namely, [1,2] and [2,1]. When  $m = 3$ , only  $m! = 6$  OPs are possible, namely, [1,2,3], [1,3,2], [2,1,3], [2,3,1], [3,1,2], and [3,2,1]. However, when  $m = 5$  and 6, 120 and 720 OPs will be generated, respectively.

A very small  $m$  makes the process sequence too simplified for OP analysis, while a very large  $m$  will generate too many OPs, thus increasing the computational effort and makes these OPs unsuitable for short time series analysis (Li et al., 2023). Therefore, this paper focuses on the case of order  $m = 4$ . Fig. 2 illustrates  $m! = 24$  kinds of OPs when  $m = 4$ .

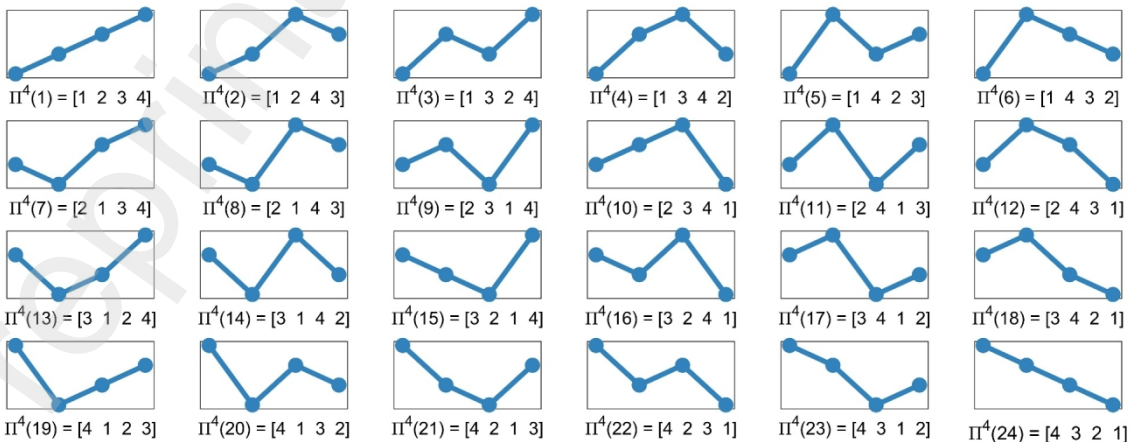


**Fig. 2.** The  $m! = 24$  kinds of OPs when  $m = 4$ .

The OP analysis divides the CCP data of length  $N$ ,  $Y = [y_1, y_2, \dots, y_N]$  into  $n$  subsequences of length  $m$ ,  $Y_i = [y_i, y_{i+\tau}, \dots, y_{i+(m-1)\tau}]$ ,  $i=1,2,\dots,n$ , where  $n$  is the number of subsequences,  $n = N - (m - 1)\tau$ .  $Y_i$  is arranged in a descending order and mapped to the corresponding OP:

$$Y_i^{m,\tau} = [y_i, y_{i+\tau}, \dots, y_{i+(m-1)\tau}] \Rightarrow \pi_i^{m,\tau} = [r_1, r_2, \dots, r_m] \quad (2)$$

where  $\pi_i^{m,\tau}$  is the corresponding OP of  $Y_i^{m,\tau}$  under parameters  $m$  and  $\tau$ , and  $\pi_i^{m,\tau} \subseteq \Pi^m$ .

To ensure the uniqueness of the OP, the mapping relation needs to satisfy the following conditions.

- 1)  $r_l < r_j$ , if  $y_l < y_j$
- 2)  $r_l < r_j$ , if  $y_l = y_j$  and  $l < j$

where  $l$  and  $j$  are the element positions in  $Y_i^{m,\tau}$  and  $j, l \in \{1, \dots, m\}$ . Condition 1 ensures that the elements in the subsequence  $Y_i^{m,\tau}$  follow a descending ordering, while Condition 2 indicates that when there are equivalent elements in  $Y_i^{m,\tau}$ , the elements are sorted according to their positions to ensure the uniqueness of the OP.

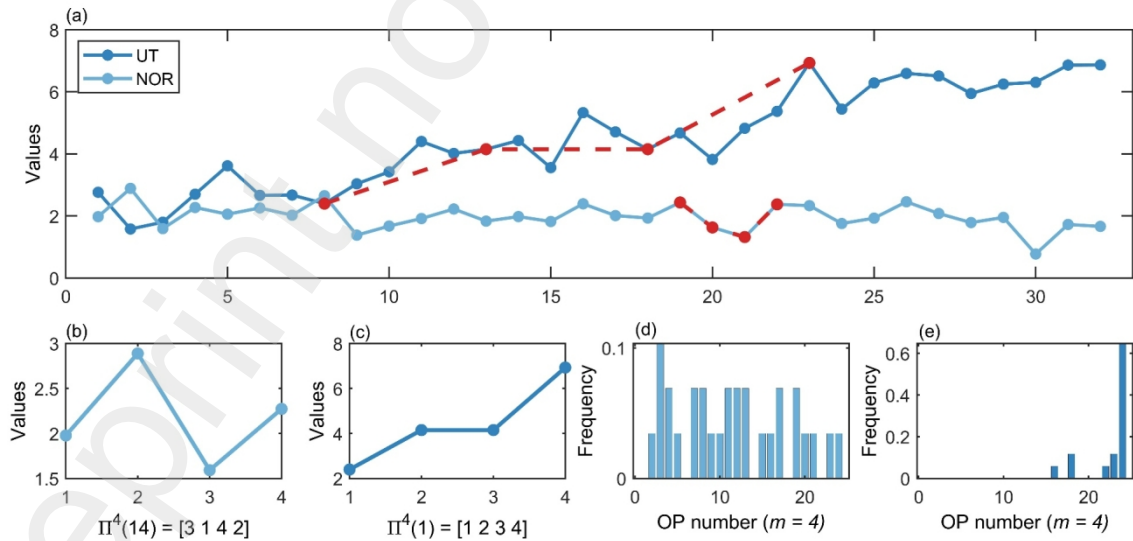


**Fig. 3.** Examples of OP feature construction for NOR and UT.

(a) NOR and UT data with length  $N = 32$ . (b) The OP of  $\pi_{19}^{4,1}$  for NOR.

(c) The OP of  $\pi_8^{4,5}$  for UT. (d) The OP features of NOR ( $m = 4, \tau = 1$ ).

(e) The OP features of UT ( $m = 4$ ,  $\tau = 5$ ).

As an example, two types of CCPs, namely, NOR and UT, of length  $N = 32$  are shown in Fig. 3(a). Let the embedding dimension parameter be  $m = 4$ . For NOR data, when  $\tau = 1$  and  $i = 19$ ,  $Y_{19}^{4,1} = [y_{19}, y_{20}, y_{21}, y_{22}] = [2.43, 1.63, 1.32, 2.37]$ . The element relationship is  $y_{21} < y_{19} < y_{22} < y_{20}$ . For UT data, when  $\tau = 5$  and  $i = 8$ ,  $Y_8^{4,5} = [y_8, y_{13}, y_{18}, y_{23}] = [2.39, 4.16, 4.31, 6.93]$ , the element relationship is  $y_8 < y_{13} < y_{18} < y_{23}$ . Both are mapped to OPs as shown in Figs. 3(b) and (c), respectively.

$$\text{NOR: } Y_{19}^{4,1} = [2.43, 1.63, 1.32, 2.37] \Rightarrow \pi_{19}^{4,1} = [3, 1, 4, 2] \Rightarrow \Pi^4(14).$$

$$\text{UT: } Y_8^{4,5} = [2.39, 4.15, 4.15, 6.93] \Rightarrow \pi_8^{4,5} = [1, 2, 3, 4] \Rightarrow \Pi^4(1).$$

All subsequences in the two CCPs are converted into OPs, and the frequency of each OP type  $\Pi^m(k)$  is counted.

$$op_k^{m,\tau} = \frac{\sum_{i \leq n} I_{u:type(u)=\Pi^m(k)}(Y_i^{m,\tau})}{\sum_{i \leq n} I_{u:type(u) \in \Pi^m}(Y_i^{m,\tau})} \quad (3)$$

where  $I_{A(u)}$  represents the indicator function of set  $A$  for counting the number of specified OP types in the CCP data.

$$I_{A(u)} = \begin{cases} 1 & \text{if } u \in A \\ 0 & \text{if } u \notin A \end{cases} \quad (4)$$

The OP features  $OP(m,\tau)$  are represented as the probability vectors of various types of OPs in the CCP under a specific embedding dimension  $m$  and time delay  $\tau$ :

$$OP(m,\tau) = [op_1^{m,\tau}, op_2^{m,\tau}, \dots, op_k^{m,\tau}, \dots, op_m^{m,\tau}] \quad (5)$$

Figs. 3 (d) and (e) present the OP features of NOR ( $m = 4$ ,  $\tau = 1$ ) and UT ( $m = 4$ ,  $\tau = 5$ ), respectively. A huge difference can be observed in the distribution of OP features between

them, thereby suggesting that these features in distinguishing different CCPs. When the data length  $N$  is sufficiently large, the probability of any OP type of NOR is  $1/24$  ( $m = 4$ ).

### 2.2.2 WOP features

The OP feature only considers the order relationship between CCP data and ignores the magnitude characteristics of the data themselves. Meanwhile, CCPs with the same order relationship cannot be easily distinguished by OP features alone. For example, the sequences [1 2 5 8] and [2 5 8 9] correspond to OP [1 2 3 4], but their magnitude characteristics (e.g., mean and variance) are obviously different. The OP features for NOR and STR, which are white noises according to the generation formula, only show small differences.

To distinguish CCPs with similar OP features and further expand the difference between other CCPs, the magnitude characteristics of the CCP data are used to weigh the OP features, which are hereinafter called WOP features:

$$WOP(m,\tau) == [wop_1^{m,\tau}, wop_2^{m,\tau}, \dots, wop_k^{m,\tau}, \dots, wop_m^{m,\tau}] \quad (6)$$

$$wop_k^{m,\tau} = \frac{\sum_{i \leq n} W_{u:type(u)=\Pi^m(k)}(Y_i^{m,\tau})}{\sum_{i \leq n} W_{u:type(u) \in \Pi^m}(Y_i^{m,\tau})} \quad (7)$$

$$W_{A(u)} = \begin{cases} w & \text{if } u \in A \\ 0 & \text{if } u \notin A \end{cases} \quad (8)$$

where  $W_{A(u)}$  denotes the improvement of  $I_{A(u)}$ , and  $w$  is the magnitude characteristic of CCP data, which is represented by the variance in CCP data:

$$w = \frac{1}{N} \sum_{q=1}^N (y_q - \bar{Y})^2 \quad (9)$$

$$\bar{Y} = \frac{1}{N} \sum_{q=1}^N y_q \quad (10)$$

where  $\bar{Y}$  is the mean of all data points in the CCP, and  $y_q$  represents the data points in the CCP,  $q = 1, 2, \dots, N$ . The WOP features take into account the sequential and magnitude characteristics of the CCP data and contain more comprehensive information.

### 2.2.3 Multi-scale WOP features

The time delay parameter  $\tau$  is a downsampling approach that reflects the data information of CCP at different observation scales. OP analysis of time series is mainly carried out in the biosignal, finance, and meteorological fields, but a few studies have been conducted for different  $\tau$ . Most of these studies only focus on small values, such as  $\tau = 1$ , and adopt unique parameter values (Kulp and Zunino, 2014).

The CCP attributes represented by OP and WOP features at different observation scales are quite different. For example, the SYS pattern is easier to distinguish when  $\tau$  is odd, while the OP features of the trend patterns (UT and DT) are more obvious for larger values of  $\tau$ . As a result, the WOP features obtained with different delay parameters  $\tau$  show large differences in their ability to distinguish between different types of CCPs.

$WOP(m, \tau)$  only analyzes information at a single observational scale and ignores information from CCP data at other observational scales, thereby leading to loss of information in CCP data and reducing the model recognition accuracy. For this reason, the WOP features in this study are integrated and analyzed under multiple observation scales, and multi-scale WOP features are proposed to improve the recognition accuracy of various CCPs.

When extracting the WOP features of CCPs, at least one complete OP should be extracted. The maximum value of the optional  $\tau$  should satisfy Eq. (11):

$$\tau_{max} = \text{round}\left(\frac{N-1}{m-1}\right) \quad (11)$$

where  $\text{round}(\cdot)$  means downward rounding. For CCP data, at most  $\tau_{max}$  WOP feature vectors can be extracted to form multi-scale WOP features.

### **2.3. Proposed CCPR method in small shifts**

#### **2.3.1 Individual classifiers based on support vector machines**

Compared with traditional control chart recognition methods based on area rules and expert systems, AI-based CCPR methods can automatically learn typical pattern features to complete recognition and alleviate the problem of false recognition (Huang et al., 2022).

ANN and SVM are the most commonly used CCPR intelligent classifiers. ANN was initially used for the intelligent recognition of CCPR and achieves a high recognition performance (Al-Ghanim and Ludeman, 1997; Pham and Wani, 1997). However, the recognition process of ANN requires a large number of training samples, and its model structure is relatively complex (Zhao et al., 2017; Zhou et al., 2018). In recent years, SVM has been widely used in CCPR due to its strong generalization ability, small number of training samples, and short training time (Cuentas et al., 2022; Lee et al., 2022). SVM has also demonstrated its superiority over other classifiers, such as ANNs, on several occasions.

Given the above advantages, multi-class SVM is used in this study as the IC for CCPR. The inputs are OP or WOP features, while the outputs are the labels of eight types of CCPs.

#### **2.3.2 Ensemble classifier based on multi-scale features**

Ensemble classification is a learning method that combines the recognition results of multiple ICs for comprehensive diagnosis. ICs, also known as weak classifiers, may show some bias in the recognition process and lead to recognition errors (Zhang et al., 2023). EC combines multiple ICs to compensate for the errors of different ICs in the recognition space and to improve recognition accuracy. EC usually has better recognition and generalization ability than ICs, which is in line with the idea of multi-scale WOP fusion analysis in Section 2.2.3.

This study proposes an ensemble CCPR method based on multi-scale WOP features (WOP-EC). By varying the parameter  $\tau$ , the  $\tau_{\max}$  group WOP features can be obtained. Each group of WOP features is assigned one IC for learning and training, and a total of  $\tau_{\max}$  ICs are obtained. The input of each IC is the OP or WOP feature under the corresponding parameter  $\tau$ , while the output is the CCP label, denoted by  $V_i$ ,  $i = 1, 2, \dots, \tau_{\max}$ .

The fusion strategy for EC is majority voting. For the recognition results of  $\tau_{\max}$  ICs, the classification label with the most votes is selected as the final result of the WOP-EC model.

ICs are screened to improve the classification efficiency. The recognition threshold is set to  $R = 50\%$ . When the recognition rate of an IC exceeds this threshold during training, its classification result will be used for the ensemble classification. Otherwise, this IC is not used to constitute EC, and its identification result will not be accepted.

### 2.3.3 Proposed WOP-EC model

This study proposes a new WOP feature based on the sequential and magnitude characteristics of CCP data to address the small shifts problem in HQP, and the WOP feature is used for training and testing the ICs. The flowchart of the proposed WOP-EC scheme is shown in Fig. 4, which is divided into three main parts.

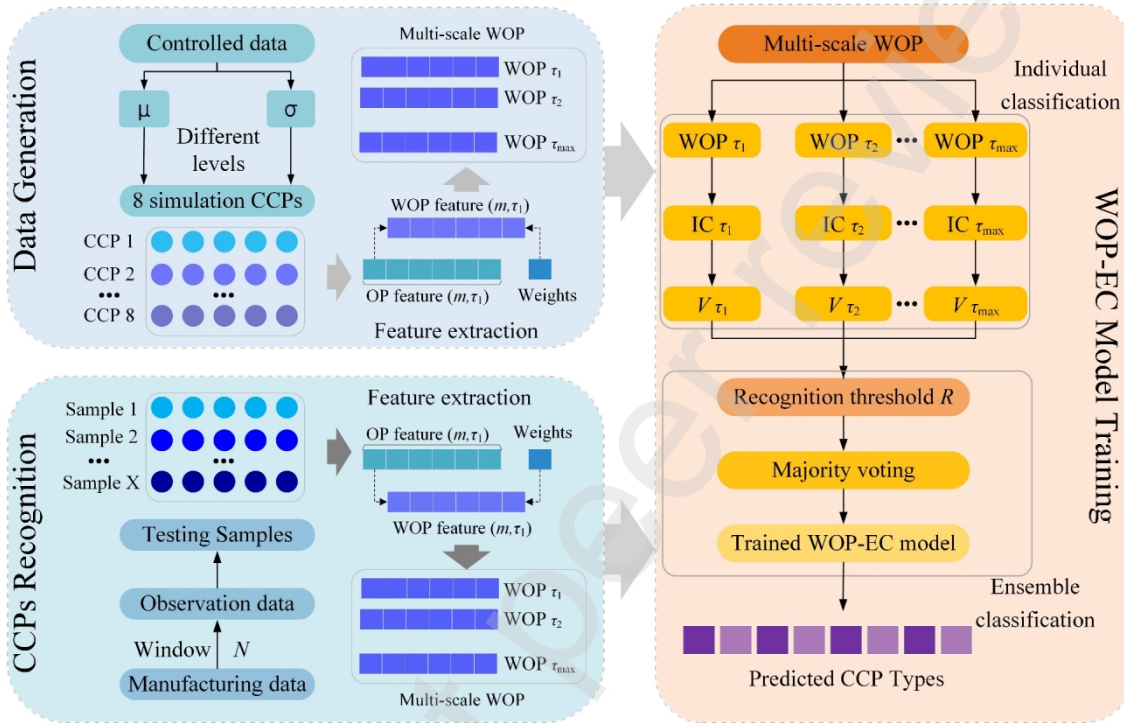


**Fig. 4.** The flowchart of the proposed WOP-EC scheme

*Part I:* Data generation. Based on the mean and standard deviation of the partially controlled process data, generate training data for eight types of CCPs at different separability levels.

*Part II:* WOP-EC model training. Vary different delay parameters  $\tau$  to extract the multi-scale WOP features of the simulated CCPs data for training  $\tau_{\max}$  ICs in the WOP-EC model.

*Part III:* CCPs recognition. Input the CCP data of the actual process under the corresponding window into the trained WOP-EC model and output the recognition results.

#### 2.3.4 Performance evaluation indicators

This study focuses on the recognition ability of the proposed WOP-EC model for eight types of CCPs at different separability levels. The recognition performance of this model is tested using the following classification indicators:

(1) Overall accurate recognition rate (ACC)

$$ACC = \frac{n_r}{N_A} \times 100\% \quad (12)$$

where  $N_A$  is the total number of CCP samples during the recognition process, and  $n_r$  is the number of correctly identified CCP samples.

(2) Type I error rate

In this paper, Type I error is caused by identifying NOR as an abnormal pattern, that is, identifying the data that are actually in a controlled process as an out-of-control state (Maged and Xie, 2023):

$$Error1 = \frac{e_1}{N_{in}} \times 100\% \quad (13)$$

where  $N_{in}$  is the total number of samples of the NOR, and  $e_1$  is the number of samples that misidentify NOR as an abnormal pattern.

(3) Type II error rate

In this paper, Type II error is caused by identifying an abnormal pattern error as NOR, that is, identifying a process that is actually already out-of-control as being in control.

$$Error2 = \frac{e_2}{N_{out}} \times 100\% \quad (14)$$

where  $N_{out}$  is the number of samples of all abnormal patterns, and  $e_2$  is the number of samples that misidentify abnormal pattern as NOR.

### 3. Experiments and results

#### 3.1 Data generation

The influence of CCP pattern parameters on recognition performance is analyzed according to the three intervals of small, moderate, and large shifts in Table 2. Given that small pattern parameters lead to poor recognition results, the small shifts interval is divided in detail in this section. Table 3 illustrates the separability levels of abnormal CCPs based on pattern parameters.

**Table 3.**  
The separability levels of abnormal CCPs.

|                    |          | Parameter range |               |               |                        |                          |
|--------------------|----------|-----------------|---------------|---------------|------------------------|--------------------------|
| Separability level |          | Amplitude $a$   | Slope $g$     | Magnitude $b$ | Random noise $\sigma'$ | Systematic departure $h$ |
| Small Shifts       | Level 1  | [0.5 0.6)       | [0.020 0.022) | [0.5 0.6)     | [0.10 0.11)            | [0.5 0.6)                |
|                    | Level 2  | [0.6 0.7)       | [0.022 0.024) | [0.6 0.7)     | [0.11 0.12)            | [0.6 0.7)                |
|                    | Level 3  | [0.7 0.8)       | [0.024 0.026) | [0.7 0.8)     | [0.12 0.13)            | [0.7 0.8)                |
|                    | Level 4  | [0.8 0.9)       | [0.026 0.028) | [0.8 0.9)     | [0.13 0.14)            | [0.8 0.9)                |
|                    | Level 5  | [0.9 1.0)       | [0.028 0.030) | [0.9 1.0)     | [0.14 0.15)            | [0.9 1.0)                |
|                    | Level 6  | [1.0 1.1)       | [0.030 0.032) | [1.0 1.1)     | [0.15 0.16)            | [1.0 1.1)                |
|                    | Level 7  | [1.1 1.2)       | [0.032 0.034) | [1.1 1.2)     | [0.16 0.17)            | [1.1 1.2)                |
|                    | Level 8  | [1.2 1.3)       | [0.034 0.036) | [1.2 1.3)     | [0.17 0.18)            | [1.2 1.3)                |
|                    | Level 9  | [1.3 1.4)       | [0.036 0.038) | [1.3 1.4)     | [0.18 0.19)            | [1.3 1.4)                |
|                    | Level 10 | [1.4 1.5)       | [0.038 0.040) | [1.4 1.5)     | [0.19 0.20)            | [1.4 1.5)                |
| Moderate Shifts    | Level 11 | [1.5 2.0)       | [0.040 0.060) | [1.5 2.0)     | [0.20 0.25)            | [1.5 2.0)                |
|                    | Level 12 | [2.0 2.5)       | [0.060 0.080) | [2.0 2.5)     | [0.25 0.30)            | [2.0 2.5)                |
| Large Shifts       | Level 13 | [2.5 3.0)       | [0.080 0.100) | [2.5 3.0)     | [0.30 0.35)            | [2.5 3.0)                |
|                    | Level 14 | [3.0 3.5)       | [0.010 0.120) | [3.0 3.5)     | [0.35 0.40)            | [3.0 3.5)                |

One dataset is collected for each separability level. Each dataset contains 8 types of CCPs, and 1000 samples are generated for each type of CCP. Among these samples, 800 are used for training, and 200 are used for testing. Therefore, for each dataset, a total of 6400 training and 1600 test samples are included. Fig.5 shows the variation of UT and NOR patterns at different separability levels.

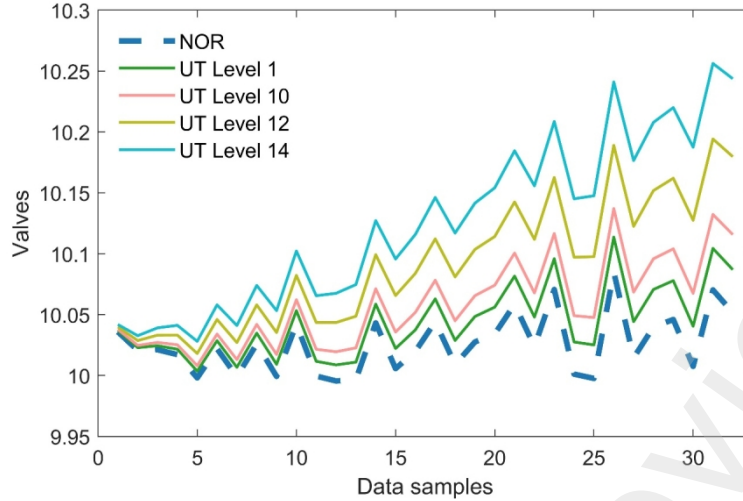


**Fig. 5.** The variation of UT and NOR patterns at different separability levels.

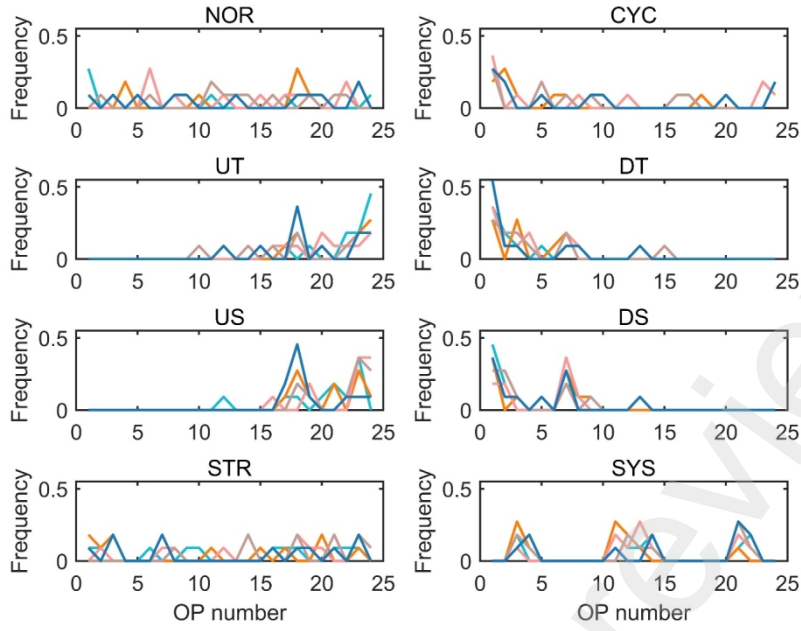
Nine different window lengths are used, starting from 16 and increasing by 8 until reaching 80. A total of 122 different classification datasets are eventually created. For the same CCPs, some differences can be observed in the recognition performance of the model with different window lengths.

### 3.2 Features extraction and analysis

#### 3.2.1 OP feature extraction

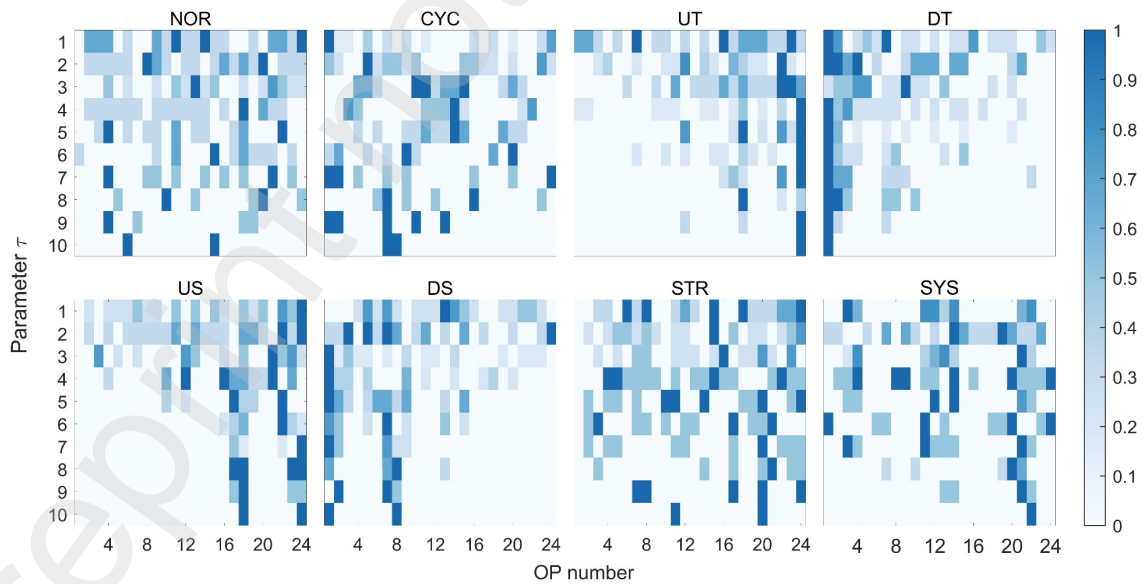
The embedding dimension  $m = 4$  is chosen for the OP analysis and discussion, and 24 possible OPs are obtained. When the window length is  $N = 32$ , the maximum delay parameter is  $\tau_{\max} = 10$ , that is,  $\tau \in [1,10]$ , according to Eq. (11).

Fig. 6 presents the distribution of OP features for CCPs at  $\tau = 7$  at Level 10. Each type of CCP contains five samples, which are represented by different colors. Large differences can be observed in the OP distributions of most CCPs, while there is some confusion for some similar CCPs, such as UT-US, DT-DS, and NOR-STR.



**Fig. 6.** The distribution of OP features for CCPs at  $\tau = 7$  in the Level 10.

The different observation scales of parameter  $\tau$  lead to large differences in the attribute expression of CCPs. To further analyze the distinguishing ability of OP features for CCPs with different  $\tau$ , all OP features corresponding to  $\tau \in [1,10]$  are converted into a heat map as shown in Fig. 7. The rows of the heat map represent a set of OP features, while the columns represent the different delay parameters  $\tau$ .



**Fig. 7.** The heat map of all OP features corresponding to  $\tau \in [1,10]$ .

When  $\tau$  is large, the OPs of the trend patterns are centrally distributed in  $\Pi^4(k_1)$ ,  $k_1 = 1$  or 24, and the OPs of the shift patterns are centrally distributed in  $\Pi^4(k_2)$ ,  $k_2 = [1,8,19,24]$ . This distribution facilitates the differentiation between trend and shift patterns. When  $\tau$  is odd, the OPs of SYS are mainly distributed in  $\Pi^4(k_3)$ ,  $k_3 = [3,4,11,12,13,14,21,22]$ , and the other OPs are almost 0. For the CYC pattern, when  $\tau = [1,2]$ , the OPs are mainly distributed in the two sides of the ordinal numbers, but when  $\tau = [3,4,5]$ , the OPs are mainly distributed in the middle ordinal numbers.

However, given that NOR and STR are essentially a set of white noise data, OP features cannot easily distinguish these two patterns.

### 3.2.2 WOP feature extraction

Accurately and comprehensively identifying all types of CCPs using only OP features is impossible. NOR and STR can be easily distinguished by their magnitude characteristics. To effectively distinguish NOR and STR and further increase the difference between other CCPs, the WOP features are obtained by weighting the OP using the magnitude characteristics of the CCP data. Fig. 8 shows all WOP features of NOR and STR when  $\tau \in [1,10]$ .

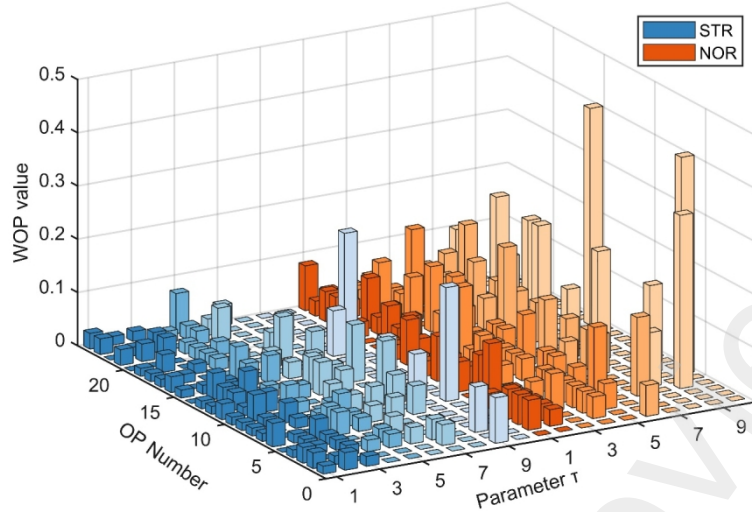


**Fig. 8.** WOP features of NOR and STR when  $\tau \in [1,10]$ .

The WOP features of STR and NOR show significant differences in their values. Therefore, the WOP features can make up for the inability of the OP feature to distinguish between STR and NOR. In addition, given that the WOP feature only changes the values of the OP feature and does not change its distribution, the difference between the other CCPs can be further expanded.

Fig. 9 illustrates the  $t$ -distributed stochastic neighbor embedding ( $t$ -SNE) results for the OP and WOP features when  $\tau = 5$  and 7. Given that the WOP feature increases the differences between similar CCPs, this feature can distinguish various types of CCPs much easier than the OP feature.

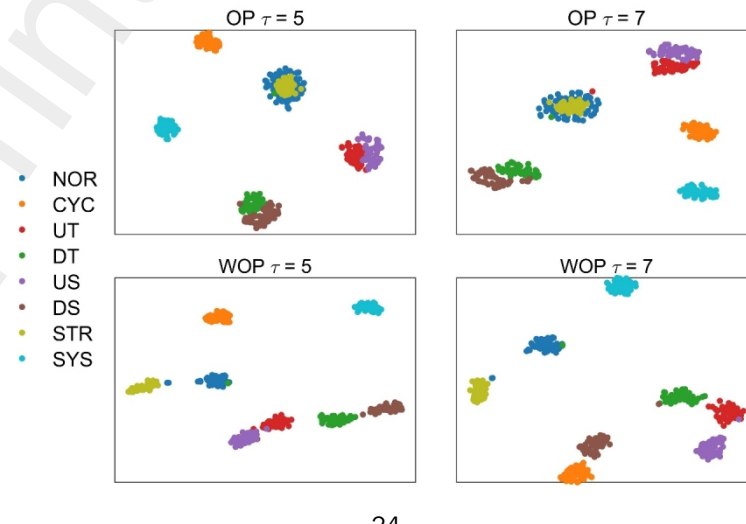


**Fig. 9.** t-SNE visualization of the OP and WOP features when  $\tau = 5$  and 7.

### 3.3 Multi-scale WOP features with ensemble classifier

SVM is chosen as the IC, whose inputs are 24-dimensional OP or WOP features and whose outputs are the predicted labels for recognizing CCPs. ICs with an ACC of less than the threshold  $R = 50\%$  are eliminated during training, and the final prediction result of the CCP to be recognized is obtained by the EC with majority voting.

The window length of CCPs is  $N = 32$ .  $\tau_{\max} = 10$  ICs are obtained when individual classification is performed for a single scale by changing the delay parameter  $\tau$ . Fig.10 shows the recognition results of ICs with OP and WOP features as input for the Levels 1, 5, 10, 12, and 14 conditions. The ACC of both OP and WOP features increases significantly along with the separability level. However, the ACC of WOP features is always higher than that of OP features, especially in moderated (Level 12: OP 80.78% and WOP 95.64%) and large shifts (Level 14: OP 83.10% and WOP 99.06%).

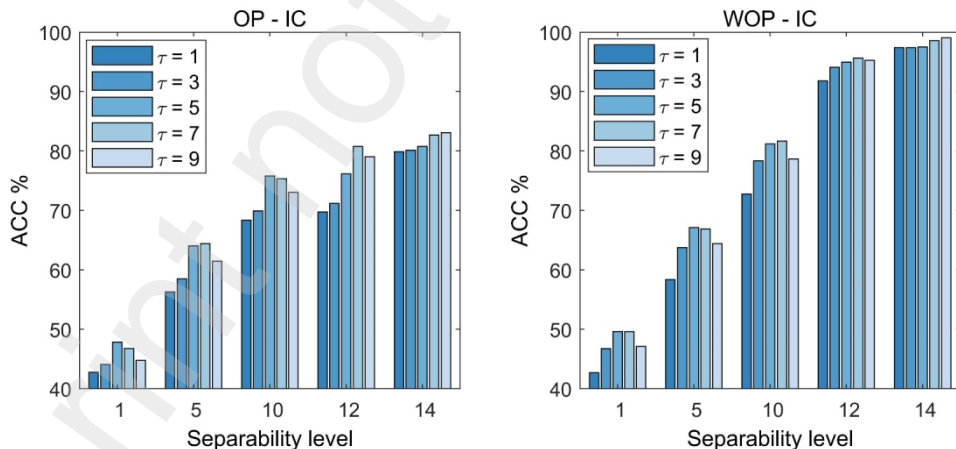


**Fig.10.** The recognition results of OP-IC and WOP-IC.

The maximum recognition results of OP and WOP features at a single scale are denoted by OP-IC and WOP-IC, respectively, whereas OP-EC and WOP-EC denote the results of multi-scale ensemble classification of OP and WOP features, respectively. Fig.11 shows

the confusion matrices of OP-IC and WOP-IC for the Levels 10 and 12 conditions. The diagonal values indicate the number of correct classifications, and the remaining values are the number of misclassifications.

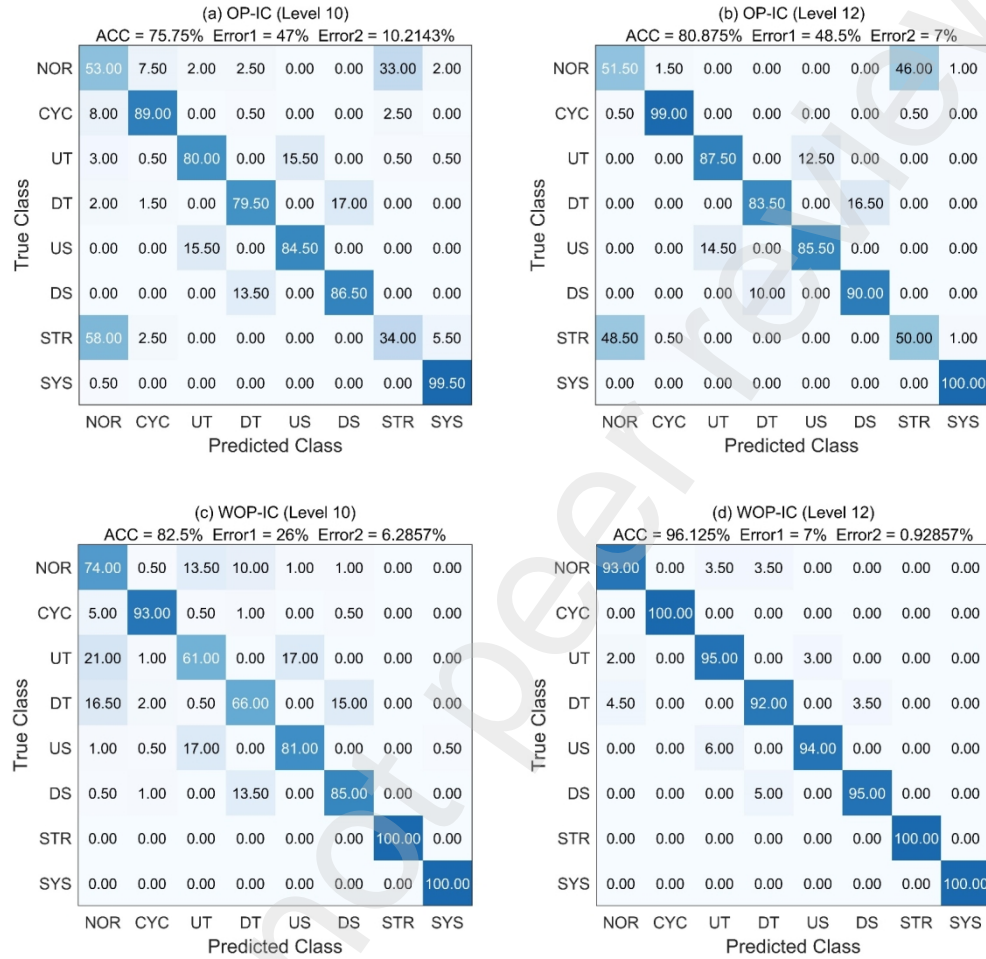


**Fig.11.** The confusion matrices of OP-IC and WOP-IC for Levels 10 and 12.

Figs. 11 (a) and (b) show the confusion matrices of OP-IC, while Figs. 11 (c) and (d) show the confusion matrices of WOP-IC. The OP feature cannot easily distinguish between NOR and STR patterns, while the WOP feature does not face this problem. When the separability level is low, both OP-IC and WOP-IC have similar pattern recognition confusions, such as UT-US and DT-DS. As the separability level increases, the ability of

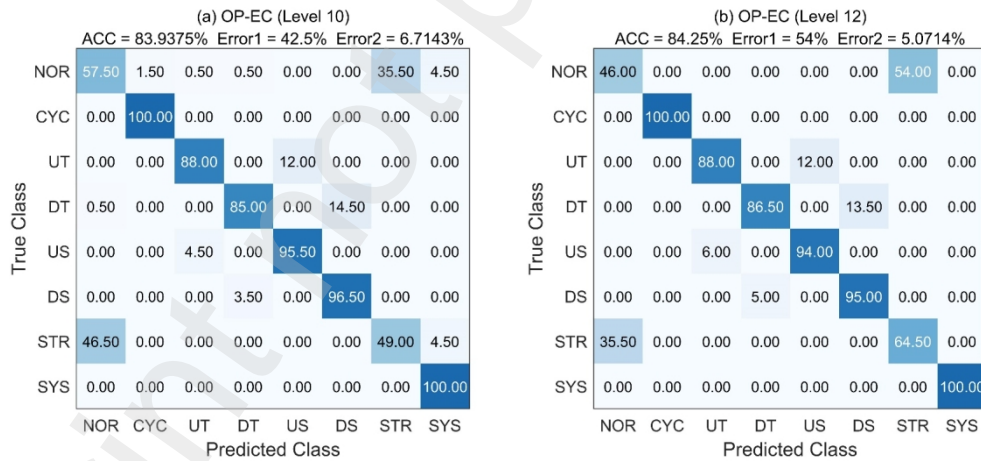
WOP-IC to distinguish similar CCPs is significantly improved, while that of OP-IC does not change much.

The WOP features with different delay parameters  $\tau$  can reflect the information of the same CCP under different observation scales. Using the idea of ensemble learning, the classification errors of different ICs are compensated by fusing multiple observation scale information to improve the model recognition performance. The recognition results of OP-EC and WOP-EC under Levels 10 and 12 conditions are shown in Table 4, while their confusion matrices are shown in Fig. 12.

**Table 4.**

The recognition performance of OP-EC and WOP-EC under Levels 10 and 12.

|            | Level 10 |       |        |              | Level 12 |       |        |              |
|------------|----------|-------|--------|--------------|----------|-------|--------|--------------|
|            | OP-IC    | OP-EC | WOP-IC | WOP-EC       | OP-IC    | OP-EC | WOP-IC | WOP-EC       |
| ACC (%)    | 75.75    | 83.94 | 82.50  | <b>94.31</b> | 80.88    | 84.25 | 96.13  | <b>99.94</b> |
| Error1 (%) | 47.00    | 42.5  | 26.00  | <b>2.50</b>  | 48.50    | 54.00 | 7.00   | <b>0.00</b>  |
| Error2 (%) | 10.21    | 6.71  | 6.28   | <b>3.71</b>  | 7.00     | 5.07  | 0.93   | <b>0.00</b>  |



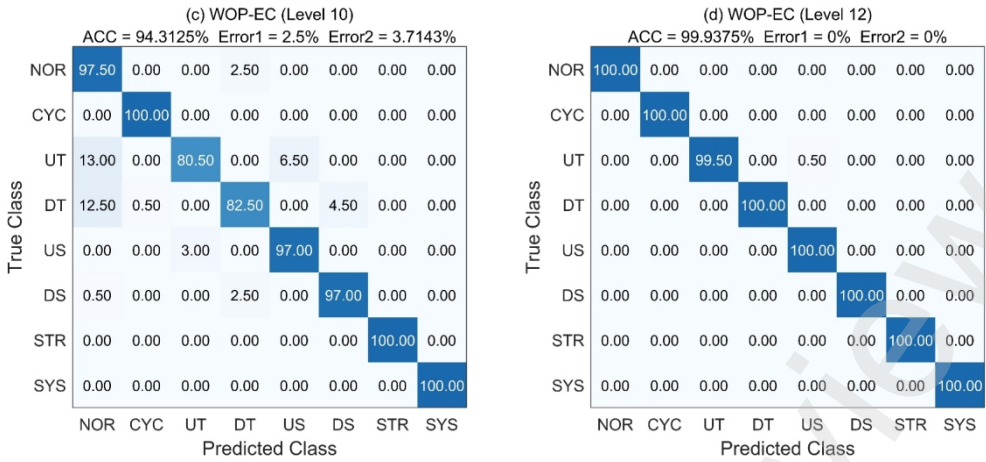


**Fig.12.** The confusion matrices of OP-EC and WOP-EC for Levels 10 and 12.

The results of OP and WOP features for Level 10 are compared in Figs. 11 and 12, which show that the OP feature cannot distinguish between NOR and STR, thereby resulting in a large Type I error (47.00% for OP-IC and 42.5% for OP-EC) with an ACC of below 90% and a high Type II error (10.21% for OP-IC and 6.71% for OP-EC). The WOP feature effectively reduces the Type I error (26.00% for WOP-IC and 2.50% for WOP-EC) and Type II error (6.28% for WOP-IC and 3.71% for WOP-EC), and significantly improves the model ACC. For the Level 12 condition, the ACC in WOP-EC is 99.94%, while that in OP-EC is only 84.25%.

In conclusion, WOP features have better recognition performance than OP features, and EC is better than IC. Therefore, the proposed multi-scale WOP-EC model can greatly improve the correct recognition performance of CCPR.

#### 4. Analysis and discussion

In this section, the proposed WOP-EC model is verified to have high robustness in terms of separability level and window length, especially in small shifts. The recognition

performance of the proposed OP and WOP features is compared with that of other common CCPR features to demonstrate their superiority.

#### 4.1 The effect of different separability levels on recognition performance

To verify the high recognition performance of the proposed WOP-EC model under small shifts, in this experiment, the CCP parameters are divided into 14 separability levels as shown in Table 3. Levels 1–10 correspond to small shifts, Levels 11–12 correspond to moderate shifts, and Levels 13–14 correspond to large shifts of CCP parameters. According to the above steps, the recognition results at each level with data length  $N = 32$  are obtained. Each group of experiments is performed 10 times and the average value was obtained. Fig. 13 shows the ACC results for the four models OP-IC, OP-EC, WOP-IC, and WOP-EC.

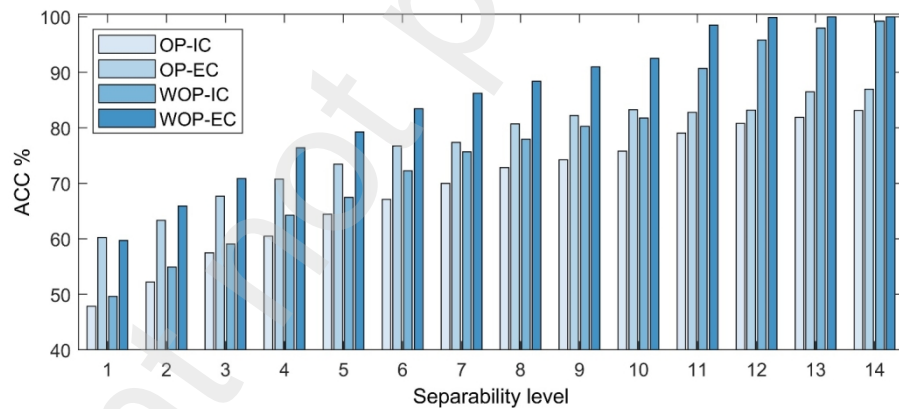


**Fig. 13.** The ACC results for the four models at different separability levels.

The ACC of the CCPR model with four feature–classifier combinations is significantly improved as the separability level increased. At low levels, the ACC difference between the WOP and OP features is small, while the ACC of EC is about 10% higher than that of ICs. When the separability level continues to increase, the ACC of WOP features

continues to increase, and the ACC of the WOP-EC model can reach 100%. However, due to the confusion of NOR and STR, the ACC of OP-EC stabilizes at 87.5%.

When the separability level is at small shifts, the ACC of OP-EC is higher than that of WOP-IC, thereby suggesting that multi-scale ensemble classification is highly beneficial in improving model recognition performance at low levels. When the separability level is at moderate and large shifts, the ACC of WOP-IC is higher than that of OP-EC, and the gap between WOP-IC and WOP-EC decreases along with increasing level. These results suggest that the differences in the attributes of various types of CCPs significantly increases at high levels, and accurate differentiation can be achieved with single scale information.

Fig. 14 shows the Type I error and Type II error of OP and WOP features at different separability levels. At any level, WOP-EC has the lowest Error1 and Error2. The Type I error of WOP features is lower than that of OP features in all cases. However, the Type II error of WOP-IC is higher than that of OP-EC when the level is low.

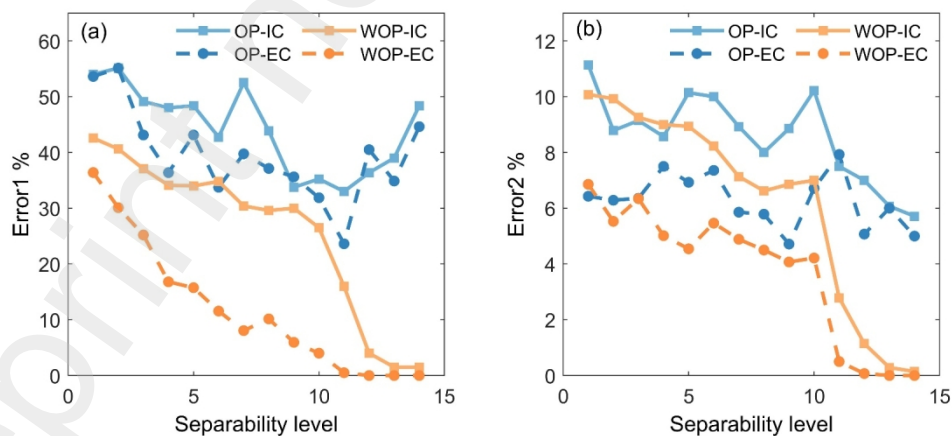


**Fig. 14.** The Type I error and Type II error of OP and WOP features at different separability levels.

During the recognition process, the OP feature incorrectly identifies a large number of NOR as STR, resulting in a high Type I error. The WOP feature contains the sequential and magnitude characteristics of CCP data, which can effectively distinguish various CCPs. The Type I error of the WOP feature decreases as the level rises and reaches 0% under moderate and large shifts.

In summary, the CCPR model (WOP-EC) combining WOP features with multi-scale EC can greatly improve the recognition ACC and effectively reduce the Type I error and Type II error at different separability levels.

#### 4.2 The effect of window length on recognition performance

The window length of CCP directly affects the recognition accuracy of features or classifiers (Ünlü, 2021), and selecting a suitable window is conducive to detecting abnormal CCPs timely and accurately. The effects of different window lengths on the recognition performance of the proposed WOP-EC model are then compared in this section, and the appropriate length for balancing recognition accuracy and efficiency is identified. Du et al. (2013) compared the computation time of samples with different window lengths and showed that the difference in computation time is small when  $N < 100$ . In this experiment, nine different window sizes with lengths ranging from 16 to 80 (incremented by 8) are considered.

Fig. 15 shows the variation of ACC with window length  $N$  for the four models at different separability levels. The ACC of the four models significantly increases as the window length  $N$  increases at any level. The ACC increases along the diagonal in Fig. 15, indicating that the model recognition performance improves as the separability level and

window length increase. The comparison results also show that the ACC of multi-scale EC is much higher than that of single-scale IC.

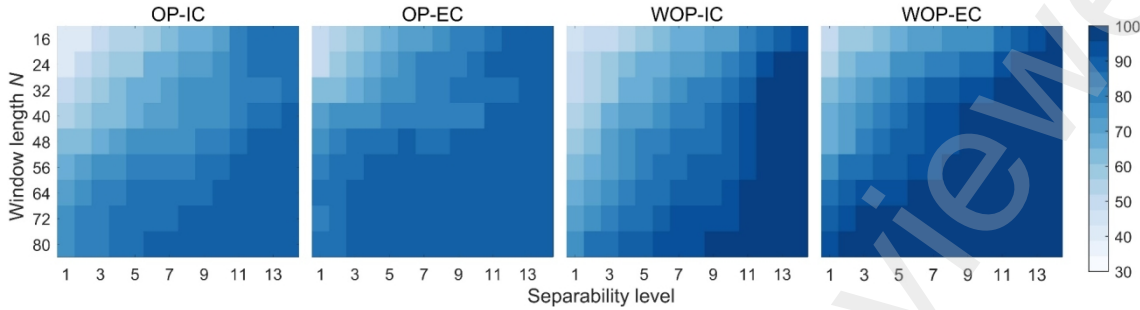


**Fig. 15.** The variation of ACC with window length  $N$ .

Figs. 16 and 17 show the Type I error and Type II error for the four proposed models. Error1 and Error2 of the OP features are only slightly affected by the separability level and window length  $N$ , while those of the WOP features are greatly affected. When the separability level is large enough or the window length is long enough, WOP-IC and WOP-EC no longer cause Type I error and Type II error.

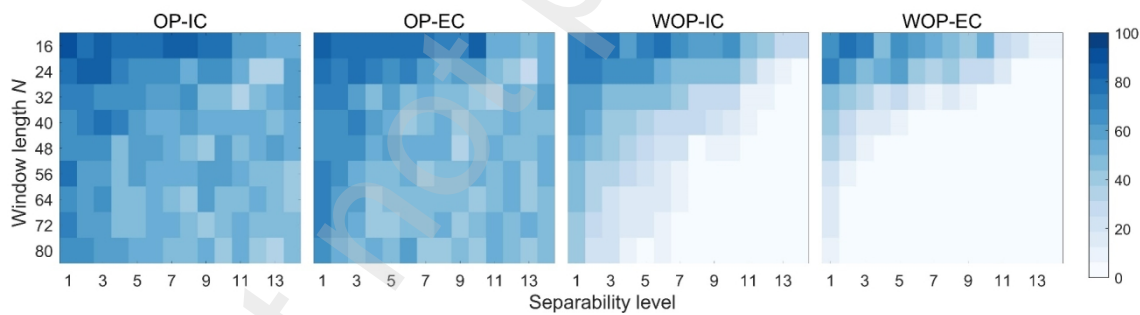


**Fig. 16.** The variation of Error1 with window length  $N$ .

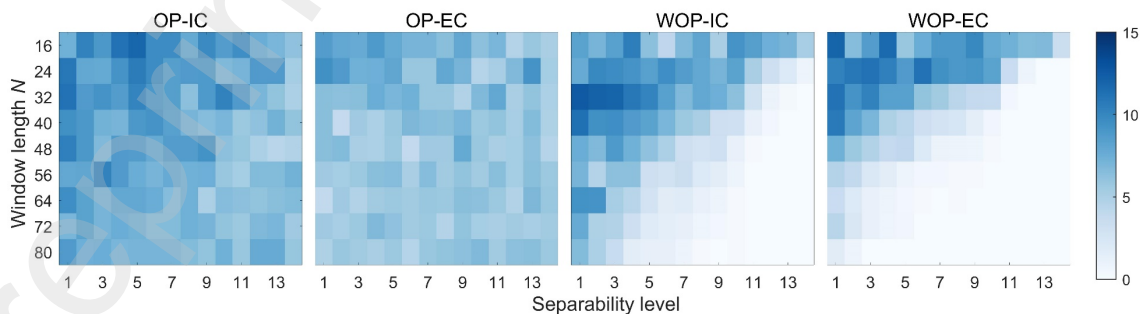


**Fig. 17.** The variation of Error2 with window length  $N$ .

Larger window sizes can contain more information and expose the attributes of CCP to the classifier. Increasing the window length can improve the recognition performance, but a very long window will reduce the recognition efficiency. Despite obtaining the recognition result more quickly, a small window is likely to cause Type I and Type II errors.

Therefore, according to the separability level of process quality data, selecting an appropriate window length should be selected to balance the recognition accuracy and efficiency of the CCPR model. When the CCP parameters are at a high separability level, a window length of  $N \geq 32$  is recommended, while at a low separability level, a window length of  $N \geq 56$  is most appropriate.

#### 4.3 Comparison with other features

In this paper, two new features are proposed, namely, 1) the OP feature based on the sequential characteristics of CCP data, and 2) the WOP feature that integrates the sequential and magnitude characteristics of CCP data. To analyze the superiority of the proposed features in distinguishing various types of CCPs at different separability levels, especially small shifts, these features are compared with other commonly used features for CCPR, including six statistical features (Hassan et al., 2003), nine shape features (Pham and Wani, 1997), statistical-shape mixed (MIX) features (Aziz Kalteh and Babouei, 2020) and wavelet (WAVE) features (Al-Assaf, 2004). The feature formulas can be found in the relevant literature.

This experiment only compares the recognition performance of different features, and different feature sets use SVM with the same training parameters as OP and WOP features as classifiers. The Error1, Error2, and ACC for these features are shown in Fig.18.

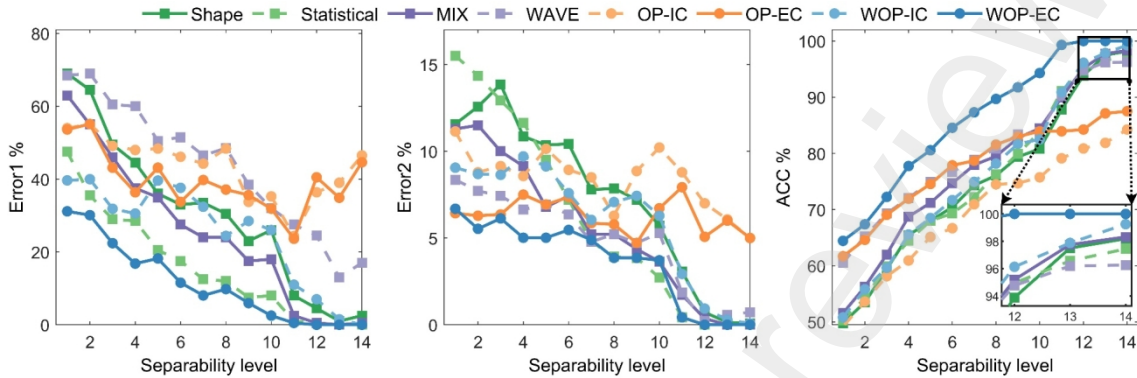


**Fig.18.** The recognition performance of different features.

The ACC values of WAVE, OP-EC and WOP-EC are significantly higher than those of the other features at low separability level. As the level increases, the ACC values of OP-EC and OP-IC gradually stabilize at 87.5%, while those of the other features increase to more than 95%. WOP-EC obtains the highest ACC at all separability levels, which can reach 100% at high levels. WOP-EC is followed by OP-EC, WOP-IC, and MIX features. The OP-EC and MIX features can be chosen for low levels, and WOP-IC and MIX features can be chosen for high levels. The worst is OP-IC, which cannot easily distinguish between NOR and STR based on sequential characteristics only.

In terms of Type I error, the best feature is WOP-EC, whose Error1 is consistently the lowest across all levels, and even reaches 0 at high levels. WOP-EC is followed by the statistical feature, whose Error1 drops to 0% in the Levels 12–14. OP-IC and OP-EC have high Error1 due to their inability to accurately distinguish between NOR and STR. The Error1 of WAVE is also high across all levels.

In terms of Type II error, the Error2 of WOP-EC is slightly higher than that of statistical features in Level 10, but is consistently the lowest in the other levels. Meanwhile, the Error2 of statistical features is highest at low levels but decreases significantly along with the separability level. OP-IC and OP-EC are almost unaffected by the separability level but are not suitable for use at high levels.

The evaluation indicators of the eight features and models at Levels 10 and 12 are shown in Table 5.

**Table 5.**

The recognition performance of eight features and models.

|          | Indicators (%) | Shape | Statistical | MIX   | WAVE  | OP-IC | OP-EC | WOP-IC | WOP-EC       |
|----------|----------------|-------|-------------|-------|-------|-------|-------|--------|--------------|
| Level 10 | ACC            | 79.38 | 83.81       | 82.75 | 83.38 | 75.75 | 83.94 | 82.50  | <b>94.31</b> |
|          | Error1         | 23.00 | 7.5         | 17.5  | 38.5  | 47.00 | 42.5  | 26.00  | <b>2.50</b>  |
|          | Error2         | 7.21  | <b>3.51</b> | 4.36  | 4.71  | 10.21 | 6.71  | 6.28   | 3.71         |
| Level 12 | ACC            | 93.88 | 94.94       | 95.19 | 94.75 | 80.88 | 84.25 | 96.13  | <b>99.94</b> |
|          | Error1         | 4.50  | 0.50        | 0.50  | 24.5  | 48.50 | 54.00 | 7.00   | <b>0.00</b>  |
|          | Error2         | 0.71  | <b>0.00</b> | 0.36  | 0.21  | 7.00  | 5.07  | 0.93   | <b>0.00</b>  |

Fig. 19 shows the confusion matrices for the four feature sets at Level 10. Compared with Figs. 11–12 and Table 4, the proposed WOP-EC has the best recognition performance. The ACC of the other common CCPR features at the high separability levels is comparable to that of the single scale WOP-IC, but the Error1 and Error2 of statistical features are lower. The Error1 of WAVE is also too high for practical process monitoring.

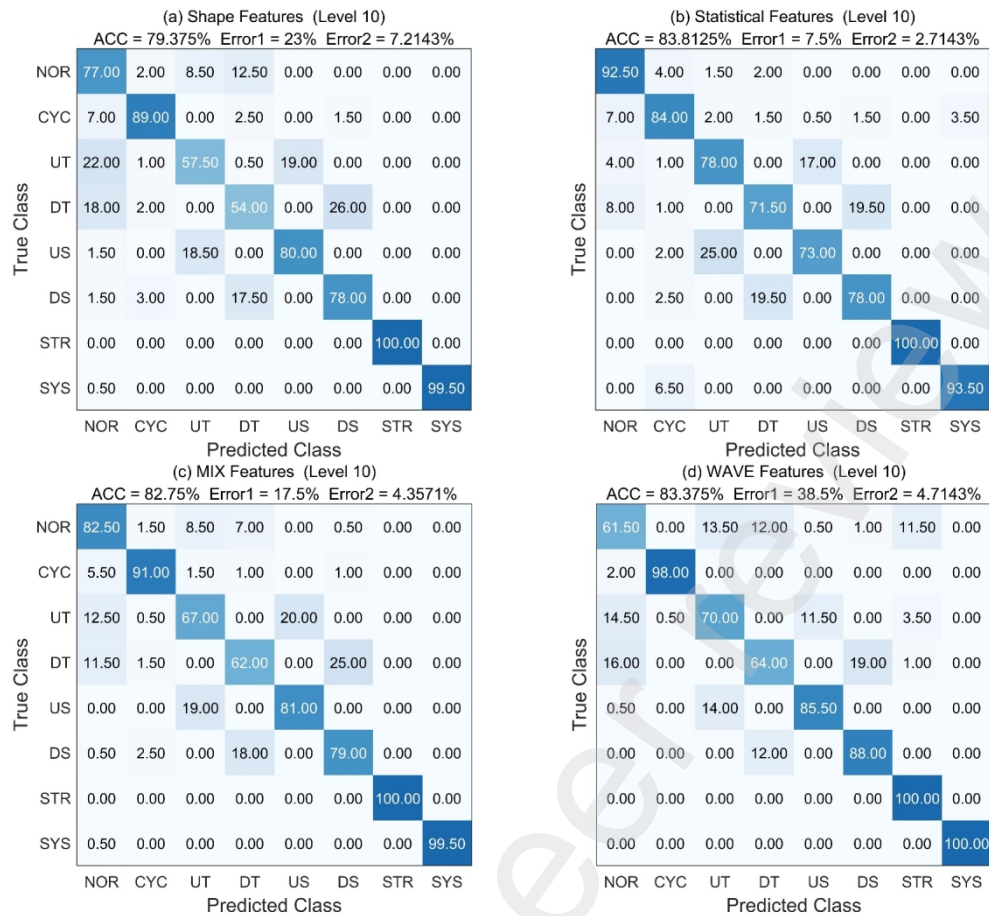


**Fig.19.** The confusion matrices of the four common feature sets in the Level 10.

In summary, the CCP recognition performance of the proposed WOP-EC feature not only maintains or even exceeds that of other commonly used features at high separability levels (moderate and large shifts), but also has a greater advantage at low distinguishable levels (small shifts).

#### 4.4 Comparison with other methods

Considering the large differences in the number of CCPs, window length, classifier type, classifier parameters, and generation parameters of CCPs across different studies, directly comparing different CCPR methods can be difficult. This paper only presents the conclusions of other research, which mostly have CCP parameters in moderate and large

shifts. The ACC of the proposed WOP-EC model in these shifts is the average of Levels 11 to 14. Table 6 compares the proposed method with the other features in the literature.

**Table 6.**  
Summary of some CCPR studies in the literature.

| Ref. (Year)                     | Inputs                                    | Separability levels     | Window Length | No. CCPs | Classifier          | ACC (%) |
|---------------------------------|---|-------------------------|---------------|----------|---------------------|---------|
| (Pham and Wani, 1997)           | Shape features                            | Moderate & Large shifts | 60            | 6        | ANN                 | 99.00   |
| (Hassan et al., 2003)           | Statistical features                      | Moderate shifts         | 20            | 6        | ANN                 | 96.79   |
| (Al-Assaf, 2004)                | WAVE features                             | Large shifts            | 32            | 6        | ANN                 | 90.15   |
| (Gauri and Chakraborty, 2006)   | Shape features                            | Moderate & Large shifts | 32            | 8        | ANN                 | 96.13   |
| (Gauri and Chakraborty, 2009)   | Shape features                            | Moderate & Large shifts | 32            | 8        | ANN                 | 96.66   |
| (Ranaee et al., 2010)           | Shape & Statistical features              | Moderate & Large shifts | 60            | 6        | PSO-SVM             | 99.58   |
| (Bag et al., 2012)              | Shape features                            | Moderate & Large shifts | 32            | 9        | Expert system       | 95.21   |
| (Du et al., 2013)               | Wave feature                              | Large shifts            | 64            | 8        | P-SVM               | 98.97   |
| (Ebrahimzadeh et al., 2013)     | Shape & Statistical features              | Moderate & Large shifts | 60            | 6        | MLP-SVM             | 99.51   |
| (Addeh et al., 2014)            | Shape & Statistical features              | Moderate & Large shifts | 60            | 6        | RBFNN               | 99.58   |
| (Zhao et al., 2017)             | Shape & Statistical features              | Moderate & Large shifts | 40            | 7        | SVM                 | 99.42   |
| (Addeh et al., 2018)            | Shape & Statistical features              | Moderate & Large shifts | 60            | 8        | BA-RBFNN            | 99.63   |
| (Zhou et al., 2018)             | Shape & Statistical features              | Moderate & Large shifts | 30            | 6        | Fuzzy SVM           | 99.28   |
| (Wong et al., 2019)             | Shape features                            | Moderate & Large shifts | 60            | 6        | BA-MLPNN            | 99.58   |
| (Zan et al., 2020)              | Raw data                                  | Moderate & Large shifts | 25            | 6        | CNN                 | 99.30   |
| (Aziz Kalteh and Babouei, 2020) | Shape & Statistical features              | Moderate & Large shifts | 60            | 9        | CWOA-ANFIS          | 99.77   |
| (Maged and Xie, 2023)           | Raw data                                  | Large shifts            | 30            | 6        | VIS-CNN             | 99.78   |
| (Alwan et al., 2023)            | Shape & Statistical features              | Moderate & Large shifts | 24            | 6        | Ensemble Classifier | 99.05   |
| (Xue et al., 2023)              | Raw data and Shape & Statistical features | Moderate & Large shifts | 50            | 12       | CNN                 | 99.7    |
| <b>Proposed method</b>          | <b>WOP-IC</b>                             | Small Shifts            | 32            | 8        | SVM                 | 82.50   |

|        |                  |    |              |
|--------|------------------|----|--------------|
|        | (Level 10)       | 64 | 91.45        |
|        | Moderate & Large | 32 | <b>98.56</b> |
|        | shifts           | 64 | 99.80        |
|        | Small Shifts     | 32 | 94.31        |
| WOP-EC | (Level 10)       | 64 | 98.50        |
|        | Moderate & Large | 32 | <b>99.88</b> |
|        | shifts           | 64 | 100.00       |

As shown in Table 6, the input features of the CCPR model do not change much over time, and different features have high recognition accuracy. However, most studies ignore the effect of the separability level of CCP parameters on recognition accuracy. Although some works have studied the small shifts problem, they only study the binary classification, that is, the classification problem between NOR and a certain abnormal CCP type, and do not distinguish different abnormal CCPs (Ünlü, 2021).

This paper investigates the CCPR problem at different separability levels. The proposed WOP-IC and WOP-EC methods can identify eight types of CCPs with high accuracy at different separability levels and show obvious advantages over other common features or methods, especially at the small shifts.

## 5. Conclusion

To address the lack of research on small change recognition of data in the key detection link of HQP, this paper designs a new CCP feature (WOP) and a multi-scale ensemble classification model that combines with the WOP feature (WOP-EC). The CCP dataset is designed according to different separability levels of the pattern parameters, and the recognition performance of the proposed WOP-IC and WOP-EC models is verified. The effects of separability level and window length on the models are discussed and compared with other common CCPR features. Experimental results show that the proposed WOP-

EC model has the best recognition performance at any separability level compared with other features or methods. The key conclusions are summarized as follows:

- 1) The WOP-EC model not only integrates sequential and magnitude characteristics but also analyzes CCP from the multi-scale, which contains more comprehensive information than traditional features.
- 2) At a high separability level, the ACC values of WOP-EC are 99.88% and 100% at window lengths of 32 and 64, respectively. At a low separability level, the ACC of the WOP-EC is much higher than that of traditional features. Under the condition of Level 10 ( $N = 32$ ), the ACC of WOP-EC is 94.31%, while the ACC of the shape features, statistical features, MIX features, and WAVE features are 77.25%, 82.94%, 79.81%, and 81.50%, respectively.
- 3) WOP-EC significantly reduces Type I error and Type II error in CCPR. Error1 and Error2 can reach 0% at a high separability level and 2.5% and 3.71% at a low separability level (Level 10), respectively.

In this paper, a new CCP feature and multi-scale ensemble classification model is proposed, which provides a tool for quality managers to monitor process variations, especially when there are small changes in pattern parameters. However, the actual production process is more complex. This study only focuses on the problem of classifying different CCPs under a single factor. Future research will further extend the WOP-EC model to concurrent CCPR problems and study the impact of unbalanced data on the proposed model.

## References

Addeh, A., Khormali, A. & Golilarz, N.A. (2018). Control chart pattern recognition using RBF neural

- network with new training algorithm and practical features. *ISA Transactions*, 79,202-216.
- Addeh, J., Ebrahimzadeh, A., Azarbad, M. & Ranaee, V. (2014). Statistical process control using optimized neural networks: A case study. *ISA Transactions*, 53(5),1489-1499.
- Al-Assaf, Y. (2004). Recognition of control chart patterns using multi-resolution wavelets analysis and neural networks. *Computers & Industrial Engineering*, 47(1),17-29.
- Al-Ghanim, A.M. & Ludeman, L.C. (1997). Automated unnatural pattern recognition on control charts using correlation analysis techniques. *Computers & Industrial Engineering*, 32(3),679-690.
- Ali, S., Pievatolo, A. & Göb, R. (2016). An Overview of Control Charts for High-quality Processes. *Quality and Reliability Engineering International*, 32(7),2171-2189.
- Alwan, W., Ngadiman, N.H.A., Hassan, A., Saufi, S.R. & Mahmood, S. (2023). Ensemble Classifier for Recognition of Small Variation in X-Bar Control Chart Patterns. *Machines*, 11(1),115.
- Aziz Kalteh, A. & Babouei, S. (2020). Control chart patterns recognition using ANFIS with new training algorithm and intelligent utilization of shape and statistical features. *ISA Transactions*, 102,12-22.
- Bag, M., Gauri, S.K. & Chakraborty, S. (2012). An expert system for control chart pattern recognition. *The International Journal of Advanced Manufacturing Technology*, 62(1-4),291-301.
- Baik, J., Kang, H., Kang, C. & Song, M. (2011). The optimal control limit of a G-EWMAG control chart. *The International Journal of Advanced Manufacturing Technology*, 56(1-4),161-175.
- Bandt, C. (2019). Small Order Patterns in Big Time Series: A Practical Guide. *Entropy*, 21(6),613.
- Bandt, C. & Pompe, B. (2002). Permutation entropy: a natural complexity measure for time series. *Physical Review Letters*, 88(17),174102.
- Barghash, M.A. & Santarisi, N.S. (2004). Pattern recognition of control charts using artificial neural networks—analyzing the effect of the training parameters. *Journal of Intelligent Manufacturing*, 15(5),635-644.
- Berger, S., Kravtsiv, A., Schneider, G. & Jordan, D. (2019). Teaching Ordinal Patterns to a Computer: Efficient Encoding Algorithms Based on the Lehmer Code. *Entropy*, 21(10),1023.
- Chen, Z., He, Y., Cui, J., Han, X., Zhao, Y., Zhang, A. & Zhou, D. (2020). Product reliability-oriented optimization design of time-between-events control chart system for high-quality manufacturing processes. *Proceedings of the Institution of Mechanical Engineers, Part B: Journal of Engineering Manufacture*, 234(3),549-558.
- Chiu, J. & Tsai, C. (2021). On-line concurrent control chart pattern recognition using singular spectrum analysis and random forest. *Computers & Industrial Engineering*, 159,107538.
- Company, W.E. (1958). Statistical quality control handbook. Indianapolis: Western Electric Company.
- Cuentas, S., García, E. & Peñabaena-Niebles, R. (2022). An SVM-GA based monitoring system for pattern recognition of autocorrelated processes. *Soft Computing*, 26(11),5159-5178.
- Du, S., Huang, D. & Lv, J. (2013). Recognition of concurrent control chart patterns using wavelet transform decomposition and multiclass support vector machines. *Computers & Industrial Engineering*, 66(4),683-695.
- Ebrahimzadeh, A., Addeh, J. & Ranaee, V. (2013). Recognition of control chart patterns using an intelligent technique. *Applied Soft Computing*, 13(5),2970-2980.
- Gauri, S.K. & Chakraborty, S. (2006). Feature-based recognition of control chart patterns. *Computers & Industrial Engineering*, 51(4),726-742.
- Gauri, S.K. & Chakraborty, S. (2009). Recognition of control chart patterns using improved selection of features. *Computers & Industrial Engineering*, 56(4),1577-1588.
- Hassan, A. (2008-1-1). Ensemble ANN-based recognizers to improve classification of X-bar control chart

- patterns. In *2008 Industrial Engineering and Engineering Management (IEEM)* (pp. 1996-2000).
- Hassan, A., Baksh, M.S.N., Shaharoun, A.M. & Jamaluddin, H. (2003). Improved SPC chart pattern recognition using statistical features. *International Journal of Production Research*, 41(7),1587-1603.
- Huang, J., Lee, P. & Jaysawal, B.P. (2022). Multiscale Control Chart Pattern Recognition Using Histogram-Based Representation of Value and Zero-Crossing Rate. *IEEE Transactions on Industrial Electronics*, 69(1),684-693.
- Kanjilal, R. & Uysal, I. (2021). The Future of Human Activity Recognition: Deep Learning or Feature Engineering? *Neural Processing Letters*, 53(1),561-579.
- Kulp, C.W. & Zunino, L. (2014). Discriminating chaotic and stochastic dynamics through the permutation spectrum test. *Chaos*, 24(3),33116.
- Landauskas, M., Cao, M. & Ragulskis, M. (2020). Permutation entropy-based 2D feature extraction for bearing fault diagnosis. *Nonlinear Dynamics*, 102(3),1717-1731.
- Lee, P., Torng, C., Lin, C. & Chou, C. (2022). Control chart pattern recognition using spectral clustering technique and support vector machine under gamma distribution. *Computers & Industrial Engineering*, 171,108437.
- Li, Y., Dai, W., Dong, J. & He, Y. (2023). Machining process condition monitoring based on ordinal pattern analysis and image matching. *The International Journal of Advanced Manufacturing Technology*, 125(7-8),3329-3347.
- Li, Y., Dai, W., Zhu, L. & Zhao, B. (2023). A novel fault early warning method for mechanical equipment based on improved MSET and CCPR. *Measurement*, 218,113224.
- Maged, A. & Xie, M. (2023). Recognition of abnormal patterns in industrial processes with variable window size via convolutional neural networks and AdaBoost. *Journal of Intelligent Manufacturing*, 34(4),1941-1963.
- Mughal, M., Azam, M. & Aslam, M. (2018). An EWMA-DiD Control Chart to Capture Small Shifts in the Process Average Using Auxiliary Information. *Technologies*, 6(3),69.
- Pham, D.T. & Wani, M.A. (1997). Feature-based control chart pattern recognition. *International Journal of Production Research*, 7(35),1875-1890.
- Ranaee, V., Ebrahimzadeh, A. & Ghaderi, R. (2010). Application of the PSO-SVM model for recognition of control chart patterns. *ISA Transactions*, 49(4),577-586.
- Ünlü, R. (2021). Cost-oriented LSTM methods for possible expansion of control charting signals. *Computers & Industrial Engineering*, 154,107163.
- Wang, J., Shang, P., Shi, W. & Cui, X. (2016). Dissimilarity measure based on ordinal pattern for physiological signals. *Communications in Nonlinear Science and Numerical Simulation*, 37,115-124.
- Weiß, C.H. & Testik, M.C. (2023). Nonparametric Control Charts for Monitoring Serial Dependence based on Ordinal Patterns. *Technometrics*, 65(3),340-350.
- Wong, P.K., Chua, A. & Department Of Electrical And Computer Engineering, N.U.O.S. (2019). Control chart pattern identification using a synergy between neural networks and bees algorithm. *Annals of Electrical and Electronic Engineering*, 2(4),8-13.
- Xue, L., Wu, H., Zheng, H. & He, Z. (2023). Control chart pattern recognition for imbalanced data based on multi-feature fusion using convolutional neural network. *Computers & Industrial Engineering*, 182,109410.
- Yeong, W.C., Lee, P.Y., Lim, S.L., Khaw, K.W. & Khoo, M.B.C. (2021). A side-sensitive synthetic coefficient of variation chart. *Quality and Reliability Engineering International*, 37(5),2014-2033.
- Yu, J., Xi, L. & Zhou, X. (2009). Identifying source(s) of out-of-control signals in multivariate

- manufacturing processes using selective neural network ensemble. *Engineering Applications of Artificial Intelligence*, 22(1),141-152.
- Zan, T., Liu, Z., Wang, H., Wang, M. & Gao, X. (2020). Control chart pattern recognition using the convolutional neural network. *Journal of Intelligent Manufacturing*, 31(3),703-716.
- Zhang, Q., Tsang, E.C.C., He, Q. & Guo, Y. (2023). Ensemble of kernel extreme learning machine based elimination optimization for multi-label classification. *Knowledge-Based Systems*, 278,110817.
- Zhao, C., Wang, C., Hua, L., Liu, X., Zhang, Y. & Hu, H. (2017). Recognition of Control Chart Pattern Using Improved Supervised Locally Linear Embedding and Support Vector Machine. *Procedia Engineering*, 174,281-288.
- Zhou, X., Jiang, P. & Wang, X. (2018). Recognition of control chart patterns using fuzzy SVM with a hybrid kernel function. *Journal of Intelligent Manufacturing*, 29(1),51-67.